17th World Conference on Earthquake Engineering, 17WCEE

Sendai, Japan - September 13th to 18th 2020

COMBINED SEISMIC AND ENERGY RETROFIT OF RC BUILDINGS: IN-PLANE STRENGTHENING OF MASONRY INFILLS USING TEXTILE REINFORCED MORTARS

D. A. Pohoryles [(1)], D. A. Bournas [(2)]

[(1)] *Scientific Project Officer, European Commission, Joint Research Centre (JRC), Ispra, Italy.* Daniel.POHORYLES@ec.europa.eu
[(2)] *Scientific Officer, European Commission, Joint Research Centre (JRC), Ispra, Italy.* Dionysios.BOURNAS@ec.europa.eu

Abstract

Due to the ageing of the European building stock, the seismic vulnerability of existing reinforced concrete (RC) buildings with non-structural masonry infills, is paired with an inadequate energy performance of these structures. Textile reinforced mortars (TRM) combined with advanced thermal insulation materials have been identified as solution to address both issues with a single intervention. While small and medium-scale testing have demonstrated the potential of the above-mentioned solution, the need for full-scale testing on a full building model has yet to be performed. In this paper, the numerical modelling preceding a pseudo-dynamic testing campaign on a full-scale masonry-infilled RC building is presented. The prototype structure was designed to replicate the behaviour of existing seismically deficient pre-1980s buildings in Southern Europe. The structure will be tested at the European Laboratory for Structural Assessment (ELSA) reaction wall facility under a pseudo-dynamic load regime. The effect of a seismic and energy retrofit scheme using TRM and thermal insulation is investigated numerically for what concerns the seismic performance herein, by means of cyclic and dynamic analyses. It was demonstrated that TRM jacketing has high effectiveness in increasing the in-plane capacity of the prototype structure, and was found to improve the dynamic behaviour of the building, leading to reduced damage at higher earthquake intensities. Ultimately, this initial assessment highlights the potential of the TRM retrofit, but the effect of combined seismic and energy retrofitting will be explored further in the full-scale study experiment.

Keywords: textile reinforced mortar; seismic retrofit; infilled RC frames; masonry infills; experimental

1. Introduction

Empirical evidence of heavy damage observed in recent earthquakes has highlighted the vulnerability of masonry-infilled reinforced concrete (RC) structures [e.g.: 1,2]. These vulnerable masonry infilled structures however constitute one of the most typical building typologies constructed between the 1960s and 1990s in Europe [3]. Many of these were built before the introduction of modern seismic codes, putting seismic countries at risk of significant losses, both in human and economic terms. Moreover, this type of structure generally presents a poor thermal performance, causing 40% of the total EU energy consumption from residential use [4].

To address the need for fast and effective retrofit strategies targeting not only the seismic behaviour, but also the energy performance for the existing European building stock, the topic of combined seismic and energy retrofitting has gained traction in recent years [5–9]. Different materials or solutions have been proposed including the use of exoskeleton [10,11] or double-skin solutions [12], but also the use of composite materials such as textile reinforced mortars (TRM) may offer avenues for combined retrofitting [13]. Previous studies investigated the use of composite materials structural retrofitting of infilled frames to reduce the risk of brittle collapse under seismic loading [14,15]. The use of TRM combined with advanced thermal insulation materials or systems (see Fig. 1), was found particularly appropriate as a combined retrofit solution [16]. The combined application was also shown to save costs in the retrofit application and its life-cycle, hence leading to significant reductions in payback periods [7,17,18].

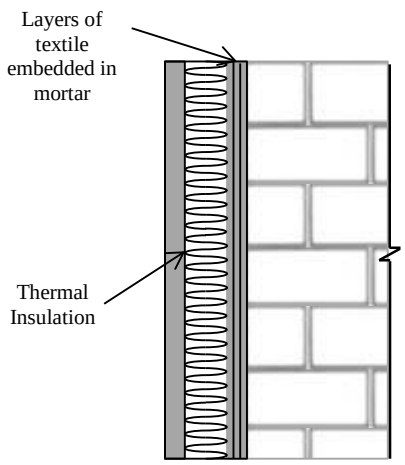

Fig. 1. Combined seismic and energy retrofit of masonry infill walls with TRM and thermal insulation.

The effectiveness of TRM jacketing on increasing the in-plane strength of masonry-infills was demonstrated experimentally on various RC frame tests. For instance, Koutas et al. [14] carried out tests on a 2/3-scaled, three-storey RC frame, which led to enhanced deformation capacity and strength increase. Further tests on full-face application found high strength increase and enhanced deformation capacities [19], particularly when mechanical interlock between textile mesh and mortar was enhanced by means of braided textiles [20,21]. However, the effectiveness of TRM jacketing in improving the in-plane seismic resistance of masonry-infilled RC frames has not yet been verified experimentally on a full-scale building.

In this study, the effect of TRM jacketing is investigated for an experimental full-scale prototype building. The building is to be tested pseudo-dynamically and numerical models for the prediction of the building response are presented in this paper. A newly developed model for TRM-strengthened infills is implemented and the effect of an increasing amount of TRM layers is first assessed by means of cyclic push-over analyses.

The effect of dynamic loading is finally examined by means of incremental dynamic analyses, highlighting the reduction in damage and hence losses at higher levels of earthquake intensity due to the retrofit.

2. Description of experimental prototype

The building of interest is an experimental structure representing a typical European pre-1980s masonry-infilled RC building. The building will be tested pseudo-dynamically at the reaction wall facility of the European Laboratory for Structural Assessment (ELSA) at the European Commission's Joint Research Centre (JRC) in Ispra. The structure, shown in Fig. 2, has four storeys with storey heights of 3m and two 4m-wide bays in the direction of testing, simulating the weak direction of the building. Only a segment of a full building is taken, with the external frames of structure in the perpendicular directions represented by the prototype. The bays in the perpendicular direction are 6m wide. Note that the first two storeys will be physically, while the upper two storeys are a numerical sub-structure during the pseudo-dynamic hybrid test [22].

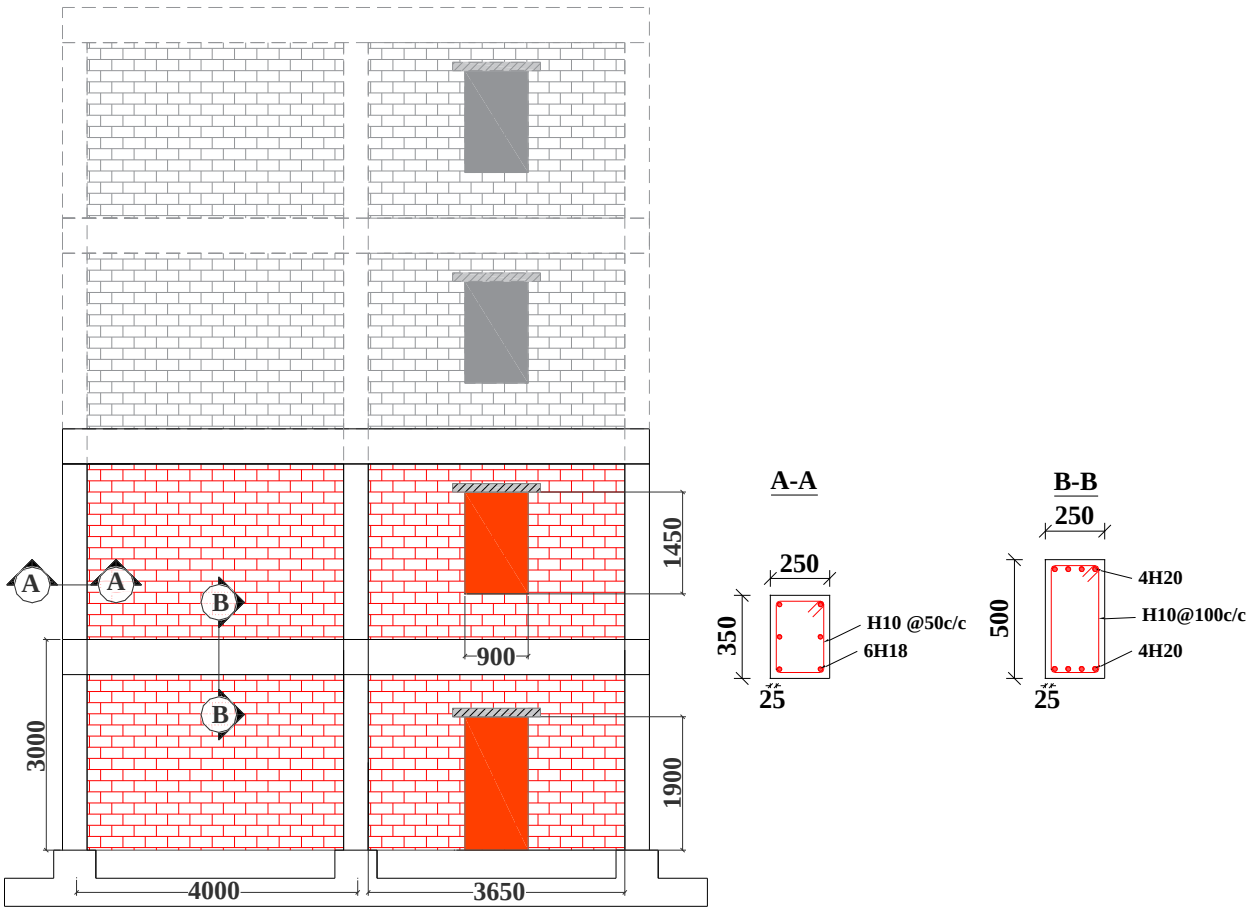

Fig. 2. Dimensions of building prototype in direction of loading and reinforcement detailing. Note: the modelled substructure is indicated in grey colour and dashed lines.

The steel reinforcement of the RC frame is over-designed in order to concentrate damage on the infills and allow for re-testing of the frame after retrofitting. The cross-sectional dimensions and reinforcement detailing for the main structural elements are detailed in Fig. 2. The dimensions of all columns is 250x350 mm and the beams are 500 mm deep, while the slab thickness is 150mm. The infill wall is made of perforated clay bricks (60 x 140 x 300 mm). The double infill walls have a total thickness equal to 120 mm

(2 x 60 mm). The opening percentage is 14.3% for the infills with windows and 18.6% for the infills with door.

The material properties are summarised in Table 1. Next to the mean compressive concrete strength (f_{cm}) and the main steel reinforcement yield strength (f_y), the brick (f_b) and mortar (f_m) compressive stengths are given and used to estiamte the infill wall strength ($f_{m,inf}$) using eq. 3.1 of Eurocode 6 [23]. For the seismic retrofit material, the TRM is assumed to consist of a textile of polymer coated E-glass fibers with a mesh size of 25 × 25 mm and a weight of 405 g/m² embedded in a strengthening mortar as described in [24]. The textile elastic modulus and TRM elastic moduli in both directions of the textile are also given in Table 1.

Table 1. Material properties

	f_{cm}	f_y	f_m	f_b	$f_{m,inf}$	E_f	E_{t1}	E_{t2}
[MPa]	35	520	12.5	11.0	3.57	73,000	520	750

3. Modelling

The rectangular reinforced concrete sections were modelled as inelastic fibre elements with plastic hinge lengths of 16.7% of the element. The confined concrete model by Mander et al. [25] and the Menegotto-Pinto model [26] were used for the concrete and steel reinforcement, respectively, while the masonry infills were modelled as diagonal compressive struts with the cyclic behaviour of the material defined using the nonlinear hysteresis rule proposed in [27]. To obtain the maximum sustained shear force, the maximum compressive stress carried by an area of infill defined from the equivalent strut width, *w*, and the actual infill thickness, t, is calculated. The strut properties were defined using the empirical equations by Mainstone [28]. To account for the openings, the strut width reduction factor developed by Asteris et al. [29] is considered. The maximum compressive stress due to corner crushing in the infills is defined by the empirical equation of Decanini et al. [30] based on the vertical infill compressive strength $f_{m,inf}$, the strut angle θ and the relative panel-to-frame stiffness λ, as given by Eq. (1):

$$f_{m\theta} = \frac{1.12 \cdot f_{m,inf} \cdot \sin\theta \cdot \cos\theta}{K1 \cdot (\lambda \cdot H)^{-0.12} + K2 \cdot (\lambda \cdot H)^{0.88}} \tag{1}$$

Where H is the storey height and K1 and K2 are empirical parameters defined based on the values of λ [30].

For the TRM-retrofitted masonry-infilled frames, a recently refined macro-model is used to assess the behaviour of the four-storey building with different amounts of retrofit. The model uses a simple strut-and-tie approach developed by Koutas et al. [31] with the tie calibrated on a large database of experiments [32]. The tie is implemented as a simple truss element with elastic material properties up to a maximum tensile force in the diagonal tie of the infill. The force developed in the tie depends on the relative orientation of the tie angle θ, angle of the fibres, α, and the angles $\theta_{cr,j}$ of an assumed multilinear stepped-crack pattern, i.e. an inclined crack (j=1) and a horizontal crack (j=2). The total force mobilised in the two axes i of the TRM fibres is then transformed geometrically into the direction of the diagonal tie as in Eq. (2) from [31]:

$$F_{tie} = \sum_{i=1}^{2}\sum_{j=1}^{2} \frac{A_{t,i}}{s_i}(\varepsilon_{te,i} \cdot E_{t,i}) \cdot d_j \cdot \left[\cot\theta_{cr,j} + (2i-3) \cdot \cot\beta_i\right] \cdot \sin\beta_i \tag{2}$$

Where, A_t is the area of TRM and E_t the elastic modulus from TRM coupon tests, β_i the angle of the fibres to the level normal to the tie-axis, s_i is the textile mesh spacing and d_j the crack lengths, both projected to the normal to the tie-axis. The effective strain developed in the textile at maximum load, ε_{te}, is expressed in

terms of the area ratio of TRM (ρ_t in %) and the square root of textile elastic modulus (E_f in MPa) using the empirical Eq. (3) developed in [32]:

$$\varepsilon_{eff} = \frac{1.40 \cdot \rho_t}{\sqrt{E_f}} \tag{3}$$

Where ρ_t is the cross-sectional area of TRM (A_t) given in Eq. 4as a fraction of the infill wall surface, determined from the height and length ($h_w \cdot l_w$):

$$\rho_t = \frac{A_t \cdot \cos\theta}{h_w \cdot l_w} \tag{4}$$

The values of the modelling parameters for the strut and tie are shown in Table 2 and Table 3, respectively. For the tie, the strengh is given for the application of 1, 2 and 3 layers of TRM. Note that the maximum axial strain in the strut, εm, is determined to be obtained at the inter-storey drift (ISD) corresponding to damage state DS3, using the definition of damage states for infilled RC frames by Cardone et al. [33] summarised in Table 4.

Table 2. Modelling parameters for the compressive strut.

Parameter	Description	Equation	Value
$f_{m,inf}$	Compressive strength of the infill	$f_{m,inf} = 0.4 \cdot f_b^{0.65} \cdot f_m^{0.25}$ [23]	3.57 MPa
$f_{m,\theta}$	Compressive strength of the strut	Eq. (1) [30]	2.88 MPa
ε_m	Axial strain at maximum (masonry)	$\varepsilon_m = \frac{\frac{l_w}{h_w} \cdot \sin\theta \cdot ISD(DS3) \cdot H}{d_m}$	0.36%
ε_u	Ultimate axial strain (masonry)	$\varepsilon_u = 5 \cdot \varepsilon_m$	1.81%
w	Strut width	$w = 0.56(\lambda \cdot H)^{-0.875} \cdot d_m$ [28]	0.95 m
w_{op}	Strut width (opening)	$w_{op} = w\,(1 - 2\alpha_w^{0.54} + 2\alpha_w^{14})$ [34]	0.38 m (window) 0.32 m (door)
α_w	Infill wall opening percentage	$\alpha_w = \frac{A_{opening}}{h_w \cdot l_w}$	14.3% (window) 18.6% (door)
θ	Strut and tie angle	$\tan^{-1}\frac{h_w}{l_w}$	34.5°

Table 3. Modelling parameters for the tensile tie.

Parameter	Description	Equation	TRM layers		
			1 layer	2 layers	3 layers
ρ_t	Area ratio of TRM	$\rho_t = \frac{A_t \cdot \cos\theta}{h_w \cdot l_w}$ [32]	1.05%	2.10%	3.15%
ε_{eff}	Effective diagonal strain in TRM	$\varepsilon_{eff} = \frac{1.40 \cdot \rho_t}{\sqrt{E_f}}$ [32]	0.17%	0.34%	0.50%
F_{tie}	Tie strength	Eq. (2) [31]	35.7 kN	142.6 kN	321.0 kN

Table 4. Damage state definition [33]

Damage state	Limit state	ISD (%)
DS1 - light	Zero Loss (ZL)	0.08 %
DS2 - moderate	Operational (OP)	0.2 %
DS3 - extensive	Damage Control (DC)	0.65 %
DS4 - partial collapse	Life Safety (LS)	1.0 %

4. Results

4.1 Cyclic time-history analysis

As a first step, the four-storey structure is analysed under cyclic loading with a cyclic displacement protocol consisting of five cycles increasing by 0.5% top-drift up to a top-drift of 2.5%. The displacement is applied at each storey following a triangular displacement pattern. Next to the as-built control building, the use of one, two and three TRM-retrofitting layers per side is investigated. The hysteresis curves for the control and TRM-strengthened models are presented in Fig. 3. The hysteresis curve of the control specimen is indicated on all curves for ease of comparison with the respective retrofit specimen. The peak base shear of 1204.9 kN for the control specimen is reached at a top-drift of 0.87%.

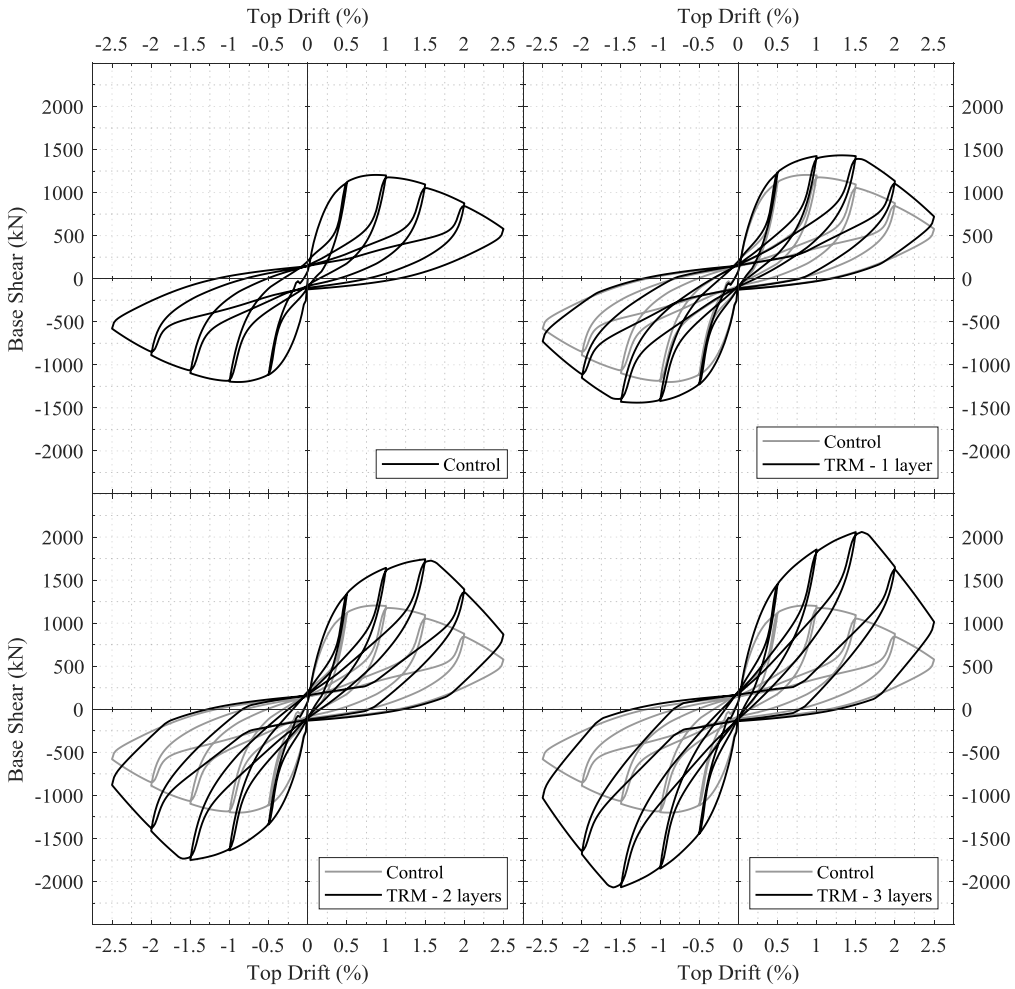

Fig. 3. Hysteresis curves from the cyclic analysis for the control and retrofitted buildings.

As shown in Table 5, in the case of the three retrofitted buildings, an increase in base shear capacity from 19.5% for one layer of TRM up to 71.7% for the three layers can be obtained. The drift at which the peak load is reached also increases significantly between the control specimen and the retrofitted specimens. With top drifts at peak between 1.3% and 1.6% for one to three layers of TRM, respectively.

Table 5. Peak response parameters for the four specimens under cyclic loading

Specimen	Peak Base Shear (kN)	Top drift at peak (%)
Control	1204.9	0.87 %
TRM – 1 layer	1439.5 (+19.5%)	1.30 %
TRM – 2 layers	1750.3 (+45.3%)	1.50 %
TRM – 3 layers	2068.6 (+71.7%)	1.60 %

It is important to note that with the chosen strut-and-tie model, the secant stiffness of the retrofitted specimens does not significantly change compared to the control specimen, as the effect of the retrofit on the strut width is ignored. Similarly, post-peak softening increases significantly for the retrofitted specimens after the peak force in the tensile tie is reached. In reality, due to improved confinement and connection of the infill with the frame, softening is expected to be reduced and the initial stiffness would be larger, this is however not captured by the model used. This aspect may be improved when considering an increase in compressive strut width due to TRM jacketing [35,36]. Still, even when ignoring this effect, the residual strength at 2.5% top-drift is enhanced for the retrofitted specimens compared to the as-built configuration.

4.2 Incremental Dynamic analysis

In order to assess the response of the building to dynamic loading, a series of fourteen earthquake records (see Table 6) has been selected and their PGA was scaled from 0.05g up to 0.6g to perform an incremental dynamic analysis [37].

Table 6. List of earthquake records used for the incremental dynamic analysis

Year	Location	Country	PGA (g)
1940	Imperial Valley (El Centro)	USA	0.32
1976	Friuli	Italy	0.48
1976	Friuli (Tolmezzo)	Italy	0.37
1979	Herceg-Novi	Montenegro	0.22
1986	Kalamata	Greece	0.29
1989	Loma Prieta	USA	0.35
1990	Roma	Italy	0.34
1994	Northridge	USA	0.37
1995	Aegion	Greece	0.52
1995	Kobe	Japan	0.82
1999	Athens	Greece	0.32
1999	Izmit (Sakarya)	Turkey	0.63
2014	Kefalonia	Greece	0.41
2015	Lefkada	Greece	0.56

As an assessment of damage, the peak inter-storey drift (ISD) is assessed at every level of PGA according to the damage state definition in Table 4. In all models, maximum inter-storey drift values were found to occur at the bottom storey of the four-storey structure. The peak ISD obtained in the incremental dynamic analysis is plotted against the intensity measure (PGA) for the four specimens in Fig. 4. The mean response from the fourteen seismic records is plotted in black. The four damage states are also indicated to highlight at which earthquake intensity different limit states are reached. It can be observed that the vulnerability of the building reduces with increased amount of retrofit layers. For the Zero Loss and Operational limit states, the difference between the control specimen and the retrofitted specimens is minor, however for the higher limit states the differences are more pronounced. As it can be seen, the average PGA required for reaching extensive damage is 0.4g, while this is higher for all three retrofitted specimens. For the three layers of TRM, DS3 is reached only at 0.46g on average. Similarly, the Life Safety limit state is reached first in the control specimen at an average PGA of 0.44g, while it is increased to 0.58g for the three layer retrofit. It is interesting to note, that while a large improvement between the single layer and double layer of TRM can be seen, the improvement in behaviour between two layers and three layers of TRM seems less pronounced. Moreover, at the larger levels of PGA, the reduction in ISD becomes increasingly pronounced for the retrofitted structure.

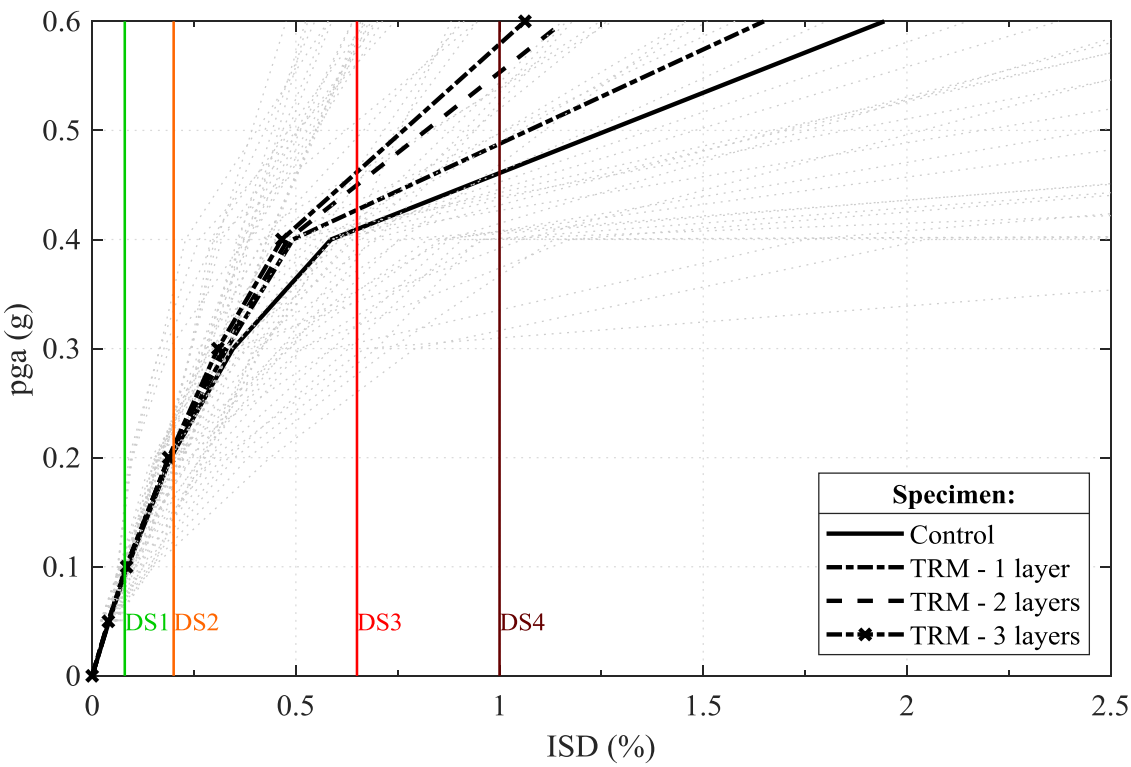

Fig. 4. Results of the incremental dynamic analysis for the control and retrofitted buildings.

The results of the IDA clearly highlight the reduced damage in the building at each level of earthquake intensity. Clearly this is also associated with a reduction in economic losses and a reduced need for repair after earthquake events. Combined with the increase in residual capacity determined in the cyclic analysis, the improvement in building safety due to the TRM retrofit is hence established. Still, it is important to note that due to modelling assumptions, the stiffness of the TRM retrofitted infilled frames is not adequately represented and models including a modification for the compressive strut parameters are required to further assess the effect of TRM retrofitting.

5. Conclusions and future work

The potential of using TRM jacketing with thermal insulation as part of a combined seismic and energy retrofitting scheme for existing RC buildings with masonry infills was investigated in this study. By means of numerical modelling, a pseudo-static cyclic analysis and an incremental dynamic analysis using fourteen earthquake records were carried out to assess the in-plane seismic behaviour of an experimental prototype RC building. It was shown that the building's base shear capacity can be significantly increased when one to three layers of TRM are applied as retrofitting material. Moreover, the dynamic analysis has highlighted the reduction in obtained inter-storey drifts for an increase in retrofit layers. This was associated to damage in the buildings and it was shown that extensive damage and partial collapse of the building occur at larger earthquake intensities for the retrofitted specimens compared to the as-built one. Future work will include the pseudo-dynamic testing of the building in the ELSA reaction wall facility (see Fig. 5), which will allow to further investigate the effect of TRM jacketing combined with advanced energy retrofitting materials, and also validate the numerical models presented in this study.

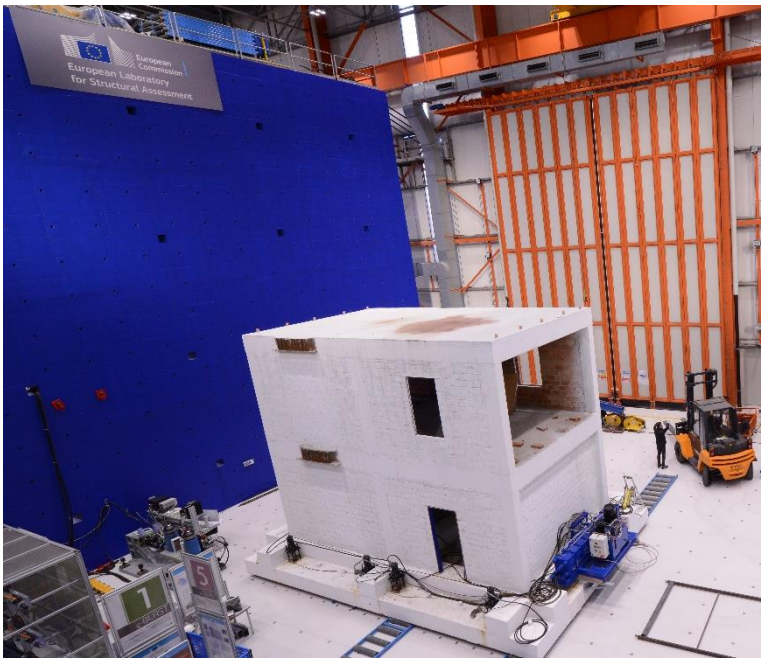

Fig. 5. Prototype structure in European Laboratory for Structural Assessment (ELSA), Joint Research Centre (JRC), European Commission.

6. Acknowledgements

The work presented was carried out under the European Commission, Joint Research Centre (JRC) Exploratory Research project iRESIST+ (Innovative seismic & energy retrofitting of the existing building stock).

7. References

[1] De Luca F, Verderame GM, Gómez-Martínez F, Pérez-García A. The structural role played by masonry infills on RC building performances after the 2011 Lorca, Spain, earthquake. Bull Earthq Eng 2014;12:1999–2026. https://doi.org/10.1007/s10518-013-9500-1.
[2] Kouris LA, Borg RP, Indirli M. The L'Aquila Earthquake, April 6th, 2009: a review of seismic damage mechanisms. Proc. Final Conf. COST Action C26 Urban Habitat Constr. Catastrophic Events, Mazzolani, FM September; 2010, p. 16–18.
[3] CTCV. Report on types of structural frames, related enclosure wall systems, and requirements for the construction systems. Portugal: Centro Tecnológico da Cerâmica e do Vidro (CTCV); 2015.
[4] Economidou M, Atanasiu B, Despret C, Maio J, Nolte I, Rapf O. Europe's buildings under the microscope. A country-by-country review of the energy performance of buildings. Buildings Performance Institute Europe (BPIE); 2011.
[5] La Greca P, Margani G. Seismic and Energy Renovation Measures for Sustainable Cities: A Critical Analysis of the Italian Scenario. Sustainability 2018;10:254. https://doi.org/10.3390/su10010254.
[6] Georgescu E-S, Georgescu MS, Macri Z, Marino EM, Margani G, Meita V, et al. Seismic and Energy Renovation: A Review of the Code Requirements and Solutions in Italy and Romania. Sustainability 2018;10:1561. https://doi.org/10.3390/su10051561.
[7] Bournas DA. Concurrent seismic and energy retrofitting of RC and masonry building envelopes using inorganic textile-based composites combined with insulation materials: A new concept. Compos Part B Eng 2018;148:166–79. https://doi.org/10.1016/j.compositesb.2018.04.002.
[8] Mistretta F, Stochino F, Sassu M. Structural and thermal retrofitting of masonry walls: An integrated cost-analysis approach for the Italian context. Build Environ 2019;155:127–36. https://doi.org/10.1016/j.buildenv.2019.03.033.
[9] Fumo M, Formisano A, Sibilio G, Violano A. Energy and Seismic Recovering of Ancient Hamlets: the Case of Baia e Latina. Sustainability 2018;10:2831. https://doi.org/10.3390/su10082831.
[10] Marini A, Passoni C, Belleri A, Feroldi F, Preti M, Metelli G, et al. Combining seismic retrofit with energy refurbishment for the sustainable renovation of RC buildings: a proof of concept. Eur J Environ Civ Eng 2017;0:1–21. https://doi.org/10.1080/19648189.2017.1363665.
[11] D'Angola A, Manfredi V, Masi A, Mecca M. Energy and Seismic Rehabilitation of RC Buildings through an Integrated Approach: An Application Case Study. Green Energy Adv 2019. https://doi.org/10.5772/intechopen.82581.
[12] Manfredi V, Masi A. Seismic Strengthening and Energy Efficiency: Towards an Integrated Approach for the Rehabilitation of Existing RC Buildings. Buildings 2018;8:36. https://doi.org/10.3390/buildings8030036.
[13] Borri A, Corradi M, Sisti R, Buratti C, Belloni E, Moretti E. Masonry wall panels retrofitted with thermal-insulating GFRP-reinforced jacketing. Mater Struct 2016;49:3957–68. https://doi.org/10.1617/s11527-015-0766-4.
[14] Koutas L, Bousias S, Triantafillou T. Seismic Strengthening of Masonry-Infilled RC Frames with TRM: Experimental Study. J Compos Constr 2015;19:04014048. https://doi.org/10.1061/(ASCE)CC.1943-5614.0000507.
[15] Koutas LN, Bournas DA. Out-of-Plane Strengthening of Masonry-Infilled RC Frames with Textile-Reinforced Mortar Jackets. J Compos Constr 2019;23:04018079. https://doi.org/10.1061/(ASCE)CC.1943-5614.0000911.
[16] Triantafillou TC, Karlos K, Kefalou K, Argyropoulou E. An innovative structural and energy retrofitting system for URM walls using textile reinforced mortars combined with thermal insulation: Mechanical and fire behavior. Constr Build Mater 2017;133:1–13. https://doi.org/10.1016/j.conbuildmat.2016.12.032.
[17] Gkournelos PD, Bournas DA, Triantafillou TC. Combined seismic and energy upgrading of existing reinforced concrete buildings using TRM jacketing and thermal insulation. Earthq Struct 2019;16:625–39. https://doi.org/10.12989/EAS.2019.16.5.625.

[18] Pohoryles DA, Maduta C, Bournas B Dionysios, Kouris LAS. Energy Performance of Existing Residential Buildings in Europe: A Novel Approach Combining Energy with Seismic Retrofitting. Energy Build under review.
[19] Selim M, Okten C, Ozkan M, Gencoglu _. Behavior of RC Frames with Infill Walls Strengthened by Cement Based Composites, International Society of Offshore and Polar Engineers; 2015.
[20] Akhoundi F, Vasconcelos G, Lourenço P, Vasconcelos G, Lourenço P. In-Plane Behavior of Infills using Glass Fiber Shear Connectors in Textile Reinforced Mortar (TRM) Technique. Int J Struct Glass Adv Mater Res 2018;2:1–14. https://doi.org/10.3844/sgamrsp.2018.1.14.
[21] Akhoundi F, Vasconcelos G, Lourenço P, Silva LM, Cunha F, Fangueiro R. In-plane behavior of cavity masonry infills and strengthening with textile reinforced mortar. Eng Struct 2018;156:145–60. https://doi.org/10.1016/j.engstruct.2017.11.002.
[22] Pegon P, Molina Ruiz Francisco J, Magonette G. Continuous Pseudo-dynamic Testing at ELSA. Hybrid Simul. Theory Implement. Appl., Leiden, The Netherlands: Taylor & Francis/Balkema; 2008, p. 79–88.
[23] CEN. BS EN 1996-1-1:2005 Eurocode 6. Design of masonry structures - Part 1-1: General rules for reinforced and unreinforced masonry structures. London: BSI; 2005.
[24] Koutas L, Pitytzogia A, Triantafillou TC, Bousias SN. Strengthening of Infilled Reinforced Concrete Frames with TRM: Study on the Development and Testing of Textile-Based Anchors. J Compos Constr 2014;18:A4013015. https://doi.org/10.1061/(ASCE)CC.1943-5614.0000390.
[25] Mander JB, Priestley MJ, Park R. Theoretical stress-strain model for confined concrete. J Struct Eng 1988;114:1804–1826.
[26] Menegotto M, Pinto PE. Method of analysis for cyclically loaded reinforced concrete frames including changes in geometry and non-elastic behavior of elements under combined normal forces and bending moment. IASBE Proc 1973.
[27] Crisafulli FJ. Seismic behaviour of reinforced concrete structures with masonry infills. PhD. University of Canterbury, 1997.
[28] Mainstone RJ. Supplementary note on the stiffness and strength of infilled frames. Curr Pap CP1374 Build Res Establ Lond 1974.
[29] Asteris PG, Cavaleri L, Trapani FD, Sarhosis V. A macro-modelling approach for the analysis of infilled frame structures considering the effects of openings and vertical loads. Struct Infrastruct Eng 2016;12:551–66. https://doi.org/10.1080/15732479.2015.1030761.
[30] Decanini LD, Fantin GE. Modelos simplificados de la mampostería incluida en porticos. Caracteristicas Stiffnessy Resist Lateral En Estado Lte Jorn Argent Ing Estructural 1986;2:817–836.
[31] Koutas L, Triantafillou TC, Bousias SN. Analytical Modeling of Masonry-Infilled RC Frames Retrofitted with Textile-Reinforced Mortar. J Compos Constr 2015;19:04014082. https://doi.org/10.1061/(ASCE)CC.1943-5614.0000553.
[32] Pohoryles DA, Bournas DA. Seismic retrofit of infilled RC frames with textile reinforced mortars: State-of-the-art review and analytical modelling. Compos Part B Eng 2020;183:107702. https://doi.org/10.1016/j.compositesb.2019.107702.
[33] Cardone D, Rossino M, Gesualdi G. Estimating fragility curves of pre-70 RC frame buildings considering different performance limit states. Soil Dyn Earthq Eng 2018. https://doi.org/10.1016/j.soildyn.2017.11.015.
[34] Asteris PG, Chrysostomou CZ, Giannopoulos I, Ricci P. Modeling of Infilled Framed Structures. In: Papadrakakis M, Fragiadakis M, Plevris V, editors. Comput. Methods Earthq. Eng., vol. 30, Dordrecht: Springer Netherlands; 2013, p. 197–224. https://doi.org/10.1007/978-94-007-6573-3_10.
[35] Pohoryles DA, Bournas DA. A unified macro-modelling approach for masonry-infilled RC frames strengthened with composite materials. Eng Struct under review.
[36] Breveglieri M, Camata G, Spacone E. Strengthened infilled RC frames: Continuum and macro modeling in nonlinear finite element analysis. Compos Part B Eng 2018;151:78–91. https://doi.org/10.1016/j.compositesb.2018.05.042.
[37] Vamvatsikos D, Cornell CA. Incremental dynamic analysis. Earthq Eng Struct Dyn 2002;31:491–514. https://doi.org/10.1002/eqe.141.

